J. Chem. Sci. (2021)133:50
https://doi.org/10.1007/s12039-021-01901-w

REGULAR ARTICLE

Theory for influence of uncompensated solution resistance on EIS of diffusion limited adsorption at rough electrode

SHRUTI SRIVASTAV, MANISH KUMAR and RAMA KANT*
Department of Chemistry, University of Delhi, Delhi 110007, India
E-mail: rkant@chemistry.du.ac.in

MS received 5 May 2020; revised 8 January 2021; accepted 26 February 2021

Abstract. Theory is developed for the electrochemical impedance spectroscopy (EIS) of the diffusion-limited adsorption process coupled with reversible charge transfer at rough electrodes under the influence of ubiquitous uncompensated solution resistance. This study quantitatively relates the impedance response of rough electrode to its phenomenological components, *viz.*, diffusion limited adsorption, reversible charge transfer and uncompensated solution resistance. The random roughness of electrode is expressed by the surface statistical property, i.e., power spectrum of roughness. The fractal nature of roughness is characterized in terms of fractal dimension, lower cut-off length and topothesy length. The high-frequency regime is controlled by the uncompensated solution resistance whereas the low-frequency regime is governed by the adsorption process. The magnitude of impedance as well as phase decreases with rise in adsorption isotherm (length) parameter. The intermediate frequency regime is controlled by the coupling of adsorption and uncompensated solution resistance with the diffusion process. The fractal roughness parameters has quantitative influence on the magnitude of impedance over whole frequency regime while the phase plot shows qualitative difference in the intermediate frequency regime. The governing length scales which controls the characteristic crossover frequencies are: diffusion length, adsorption-ohmic coupling length and topothesy length (or width of interface). The three emergent crossover frequencies are: (i) ohmic reduced inner crossover frequency (ii) adsorption roughness topothesy dependent pseudo-quasireversibility characteristic frequency (iii) outer crossover frequency.

Keywords. Diffusion-limited; adsorption; uncompensated solution resistance; rough electrode; finite fractal.

Abbreviations

K	Adsorption Isotherm Parameter
R_Ω	Uncompensated solution resistance
D_H	Haussdorff Fractal Dimension
ℓ	Lower Cut-off Length
L	Upper Cut-off Length
ℓ_τ	Topothesy Length
$L_{a\Omega}$	Adsorption-Ohmic coupling length
C_{ad}	Adsorption capacitance
L_D	Diffusion length($\sqrt{D/i\omega}$)
C_α^0	Bulk concentration of the species *e.g.* $\alpha = O, R$
δC_α	Change in concentration of species
η_0	Small Amplitude of Perturbed Potential
$\vec{K}_\parallel$	Vector (K_x, K_y)
$\hat{n}$	Normal vector drawn in outward direction
$\vec{r}_\parallel$	Vector (x, y)
Γ_α	Excess Surface Concentration
$\delta(\vec{K}_\parallel)$	Dirac delta function in wave-vector $\vec{K}_\parallel$
$\zeta(\vec{r}_\parallel)$	Arbitrary surface profile
$\hat{\zeta}(\vec{K}_\parallel)$	Fourier transform of the arbitrary surface profile
$j(t)$	Current density
$y(\omega)$	Admittance density
$Y(\omega)$	Total admittance
$Y_P(\omega)$	Smooth electrode admittance
$Y_W(\omega)$	Warburg admittance
$Y_{ad}(\omega)$	Adsorption admittance
F_1	Appell's Function
${}_2F_1$	Hypergeometric Function
$K_\parallel$	$[K_x^2 + K_y^2]^{1/2}$
δ	$D_H - 5/2$
ω_i	Inner cut-off angular frequency

*For correspondence

Supplementary Information: The online version contains supplementary material available at https://doi.org/10.1007/s12039-021-01901-w.

Published online: 06 May 2021

ω_o	Outer cut-off angular frequency
Γ	Specific volume capacitance
μ	Strength of fractality

1. Introduction

Adsorption assisted processes play dominant role in many branches of chemical and biological sciences.[1] These processes are extensively involved in the electrochemical study of adsorption assisted charge transfer on various electrode systems.[2–6] Electrochemical nature and topography of electrode surface has dominant effect on all electrochemical processes as they influence ion adsorption/desorption kinetics, mass transport and charge transfer.[7,8] These adsorption and desorption processes causes complex kinetics behavior at electrode with topographical disorder.[9,10] Geometric irregularity of the electrode surface significantly affects the adsorption assisted charge transfer processes.[11] The properties of electrode processes are also influenced by the adsorbed species which are not directly involved in the electrode reaction.[12,13]

Frumkin and Melik Gaikazyan[14] were the first to use impedance measurements for determining the adsorption kinetics based on the dynamic differential capacitance in the region of adsorption-desorption peaks. The Frumkin-Melik-Gaikazyan (FMG) model refers to an adsorption process limited by a linear semi-infinite diffusion in the absence of electrochemical reactions. Electrochemical impedance spectroscopy (EIS) is a widely used technique to derive the constituent elementary reaction steps of the electrochemical process. It is also used to extract the numerical values of the rate constants and other kinetic parameters characterizing these reaction steps.[15] The adsorption phenomenon for guanine oxidation and the shape of the impedance plots are influenced by the modified surface roughness effects, which leads to the phase angle value $< 90°$.[16] The theoretical expressions are derived for the interfacial impedance which is controlled by both diffusion and adsorption processes.[17] In electron transfer processes, the total interfacial impedance is usually resolved into diffusion-limited impedance along with the adsorption kinetics, in the presence of uncompensated solution resistance. Despite very significant experimental work carried out worldwide, it was difficult to provide an explicit expression relating the geometrical irregularity of the surface and the impedance response.[9,18]

In the last three decades, Kant and coworkers have established a series of relationships for the techniques such as chronoamperometry,[19] impedance,[20–27] chronocoulometry,[28] chronoabsorptiometry,[29] chronopotentiometry,[30] admittance voltammetry[31] and pulse voltammetry[32,33] at the randomly rough surface. These techniques result into the observable like current, admittance, absorbance and charge transients with the morphology of the electrodes through the power spectrum of the roughness.[25,26,28,29,34–40] The impedance response of diffusion-limited adsorption at the fractal electrodes has been discussed earlier,[11] wherein these studies connect the diffusion-limited adsorption phenomenon at the interface to the electrode morphology. The experimental realization of theoretical results is usually influenced by the presence of uncompensated solution resistance.[41,42] To reduce the influence of ohmic (or potential) drop, inert electrolytes or highly conducting supporting media are used. Its effect can also be reduced by minimizing the distance between the working and the reference electrode. There are two processes occurring at the interface of electrode, i.e., diffusion and adsorption, both these processes are limited by the uncompensated solution resistance. The diffusion and uncompensated solution resistance are non-linearly coupled phenomena. The subtraction of iR drop is an arbitrary approach which is a major hindrance in understanding transient influence of ubiquitous ohmic contributions to phenomena. There exist two phenomenological length scales, i.e., diffusion length $L_D = \sqrt{D/\omega}$ and adsorption-ohmic coupling length ($L_{a\Omega}$) each correspond to diffusion and adsorption process, respectively. The electrochemical response is dominantly controlled by the magnitude of these two phenomenological lengths. It is worth mentioning here that $L_{a\Omega}$ is dependent on the adsorption parameter and solution resistance while L_D is diffusion length.

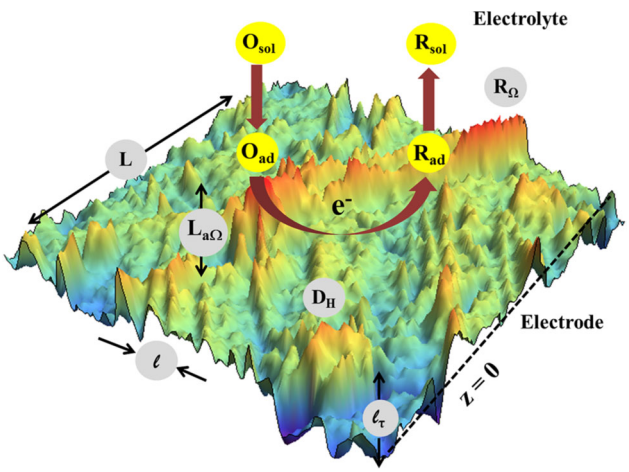

Figure 1. Schematic representation of diffusion limited adsorption process in presence of uncompensated solution resistance at randomly rough electrode.

In the present work, we wish to explore the influence of uncompensated solution resistance on the diffusion-limited adsorption process on the complex impedance response. Figure 1 represents the schematic representation of diffusion limited adsorption process in presence of uncompensated solution resistance at randomly rough electrode. This work has been segmented into various parts as (i) mathematical formalism and the boundary conditions associated with the adsorption process in the presence of uncompensated solution resistance. (ii) The perturbative approach is used to solve the expression for admittance density and total admittance at random rough surface. (iii) The generalized admittance expression is expressed in the form of surface structure factor through which roughness features are incorporated. (iv) The explicit expression of admittance is obtained for the finite fractal system. (v) Finally, the results and discussion section unravels the influence of various morphological and phenomenological parameters.

2. Formulation

Solution resistance is an important part in most electrochemical phenomena involving kinetics and diffusion process. Diffusion and uncompensated solution resistance are non-linearly coupled. Simplistic iR compensation is an adhoc approach without proper justification as phenomenon and is also a major hindrance in understanding dynamical response. Therefore, understanding the mysterious dynamic influence of uncompensated solution resistance in electrochemical systems is of utmost importance. Here we develop the admittance theory for the influence of uncompensated solution resistance in the diffusion-limited adsorption on a rough electrode.

The diffusion equation for sinusoidal perturbation, $e^{\imath\omega t}$, is simplified as

$$\imath\ \omega\ \delta C_\alpha(\vec{r}) = D_\alpha \nabla^2 \delta C_\alpha(\vec{r}) \tag{1}$$

where α stands for the oxidized (O) and reduced (R) species. D_α is the diffusion coefficient for the α-th species. ω is the angular frequency and $\imath = \sqrt{-1}$. Here $\delta C_\alpha(\vec{r},t) = C_\alpha(\vec{r},t) - C_\alpha^0$, represents the concentration difference in the interfacial $(C_\alpha(\vec{r},t))$ and bulk concentration (C_α^0). The change in concentration for initial and bulk boundary condition are: $\delta C_\alpha(\vec{r}, t=0) = 0$, $\delta C_\alpha(\vec{r}_\parallel, z\to\infty, t) = 0$, respectively. The initial and bulk boundary conditions represent that the uniform concentration of electroactive species is maintained in the solution. The adsorption rate of a substance is proportional to the diffusion flux to the electrode. The amount of species adsorbed is used as a boundary condition associated with the semi-infinite linear diffusion. The excess surface concentration (Γ_α) of adsorbable substance is given by[43]

$$\Gamma_\alpha = \int_0^t D_\alpha \left(\frac{\partial C_\alpha(\vec{r},t)}{\partial n}\right)_{z=\zeta(\vec{r}_\parallel)} dt \tag{2}$$

If the adsorption process takes place at a very fast rate then the process is completely diffusion-controlled. At this stage the surface concentration is related to the volume concentration at the electrode surface, $(C_\alpha)_{z=0}$ and the adsorption isotherm parameter. This simplification is quite justified as it is obtained from the alternating current method (EIS method).[14] Thus the kinetics of adsorption is obtained as,[44,45]

$$\Gamma_\alpha = KC_\alpha \tag{3}$$

where K is a characteristic distance in solution upto which adsorbing species are adsorbed to provide a given surface excess. Also, K is adsorption isotherm (length) parameter representing the extent of interaction between metal and species. The combination of Eq. (2) and Eq. (3) provides the boundary condition used to solve the Fick's diffusion equation. To solve the problem of diffusion-controlled adsorption impedance, the adsorption isotherm can be linearized which make the problem of diffusion-controlled adsorption solvable, i.e.,

$$\frac{\partial\Gamma_O(t)}{\partial t} + \frac{\partial\Gamma_R(t)}{\partial t} = D\left[\frac{\partial\delta C_O(\vec{r},t)}{\partial n} + \frac{\partial\delta C_R(\vec{r},t)}{\partial n}\right]_{z=\zeta(\vec{r}_\parallel)} \tag{4}$$

By equating Eq. (2) and Eq. (3), we get the expression which relates the diffusion flux and adsorption isotherm at the interface and is given by[43]

$$\int_0^t D_\alpha \left(\frac{\partial C_\alpha(\vec{r},t)}{\partial n}\right)_{z=\zeta(\vec{r}_\parallel)} dt = KC_\alpha \tag{5}$$

As the concentration varies locally, we have, $C_\alpha = \delta C_\alpha + C_\alpha^0$, then Eq. (5) can be transformed to the expression showing heterogeneity in terms of concentration. Using the Laplace transformation technique, we can transform the integral form of Eq. (1), into simple differential form, which is easy to solve and can be expressed as

$$\frac{K_O\partial\delta C_O(\vec{r},t)}{\partial t} + \frac{K_R\partial\delta C_R(\vec{r},t)}{\partial t} = D\left[\frac{\partial\delta C_O(\vec{r},t)}{\partial n} + \frac{\partial\delta C_R(\vec{r},t)}{\partial n}\right]_{z=\zeta(\vec{r}_\parallel)} \tag{6}$$

where δC_α is the function of both position vector $(r_\parallel)$

and time (t) in Laplace domain, p is Laplace transformed variable. The boundary conditions associated with diffusion-controlled adsorption problems fall into mixed boundary value problems. The linearized Nernstian boundary condition can be written as

$$\frac{\delta C_O}{C_O^0} - \frac{\delta C_R}{C_R^0} = -nf\eta(t). \tag{7}$$

where $f = F/RT$, F is Faraday's constant, R is gas constant and T is temperature. Incorporating the ohmic losses, the linearized Nernstian boundary constraint becomes,

$$\frac{\delta C_O}{C_O^0} - \frac{\delta C_R}{C_R^0} = -nf(\eta(t) - jR_\Omega), \tag{8}$$

where $\eta(t) = \eta_0 e^{\iota\omega t}$ is the perturbed electrode potential. Here η_0 is the small amplitude of sinusoidal perturbed potential. Using the expression of δC_R term obtained from Eq. (8) into Eq. (2), we get the simplified boundary condition for an arbitrary two-dimensional rough surface. Using the flux-balance condition,[38] the linearized adsorption boundary condition under Nernstian reaction[43] for the moderately supported electrolyte is obtained as (see SI-A in Supplementary Information),

$$\frac{\partial \delta C_O(\vec{r})}{\partial n} - \Lambda_{a\Omega}\delta C_O(\vec{r})|_{z=\zeta(\vec{r}_\parallel)} = {\Lambda^0}_{a\Omega} \tag{9}$$

where $\Lambda_{a\Omega} = \frac{K\iota\omega}{D(\iota\omega\Gamma K R_\Omega + 1)}$ and ${\Lambda^0}_{a\Omega} = \frac{nf\eta_0 K\iota\omega}{D(\iota\omega\Gamma K R_\Omega+1)(C_O^{-1}+C_R^{-1})}$ have dimension of $[Length]^{-1}$ and $[Length]^{-1}mole/cm^3$, respectively. Our problem, i.e., diffusion-controlled adsorption impedance in the presence of uncompensated solution resistance to the disordered electrode is similar in mathematical derivation as shown in reference.[38] Adopting the similar formalism one can find the current transient for the diffusion-controlled adsorption process in the presence of uncompensated solution resistance at the rough electrode. Under these conditions, the expression for current is given by,[38,43]

$$j(S,t) = nFD_\alpha \partial_n \delta C_\alpha(\vec{r}_\parallel, t) \tag{10}$$

To obtain current transient as a function of the boundary profile, we need to evaluate the concentration field. This concentration term can be obtained using Taylor expansion upto second order in random surface profile at the reference plane, i.e., z = 0. The second-order perturbative solution for the concentration profile in the Fourier and Laplace transformed domain at the rough surface for diffusion-controlled adsorption process is obtained as

$$\begin{aligned}\delta C(\vec{K}_\parallel, z, p) = -\frac{{\Lambda^0}_{a\Omega}}{p}[\hat{\mathcal{C}}_0 (2\pi)^2\delta(\vec{K}_\parallel) + \hat{\mathcal{C}}_1\,\hat{\zeta}(\vec{K}_\parallel) \\ + \hat{\mathcal{C}}_2\,\hat{\zeta}(\vec{K}_\parallel)(\vec{K}_\parallel - \vec{K}'_\parallel)]\end{aligned} \tag{11}$$

The operators $\hat{C}_0, \hat{C}_1$ and $\hat{C}_2$ are defined below

$$\hat{\mathcal{C}}_0 \equiv \left\{\frac{e^{-\omega_0 z}}{\omega_0 + \Lambda_{a\Omega}}\right\}$$

$$\hat{\mathcal{C}}_1 \equiv \left\{\frac{\omega_0\, e^{-\omega_\parallel z}}{\omega_\parallel + \Lambda_{a\Omega}}\right\};$$

$$\begin{aligned}\hat{\mathcal{C}}_2 \equiv \frac{e^{-\omega_\parallel z}}{(2\pi)^2}\int d^2K_\parallel{}' \Bigg\{\frac{-\omega_0^2}{2(\omega_\parallel + \Lambda_{a\Omega})} + \frac{\omega_0\omega_{\parallel,\parallel'}}{\omega_\parallel + \Lambda_{a\Omega}} \\ + \frac{\omega_0}{\omega_\parallel + \Lambda_{a\Omega}}\frac{K'_\parallel.(K_\parallel - K'_\parallel)}{\omega_{\parallel,\parallel'} + \Lambda_{a\Omega}} \\ - \frac{\omega_0}{2(\omega_0 + \Lambda_{a\Omega})}\frac{K'_\parallel.(K_\parallel - K'_\parallel)}{\omega_\parallel + \Lambda_{a\Omega}}\Bigg\}\end{aligned}$$

where $\omega_0 = (p/D)^{1/2}$, $\omega_\parallel = (\omega_0^2 + \vec{K}_\parallel^2)^{1/2}$, $\omega_{\parallel,\parallel'} = (\omega_0^2 + |\vec{K}_\parallel - \vec{K}'_\parallel|^2)^{1/2}$ and $\int d^2K_\parallel \equiv \int_{-\infty}^{\infty} dK_x \int_{-\infty}^{\infty} dK_y$. p is the Laplace transform variable and $\delta(\vec{K}_\parallel)$ is the Dirac delta function. $\hat{\zeta}(\vec{K}_\parallel)$ is the Fourier transform of an arbitrary surface profile function $\zeta(\vec{r}_\parallel)$ and is given by

$$\hat{\zeta}(\vec{K}_\parallel) = \int d^2r_\parallel e^{-\iota\vec{K}_\parallel.\vec{r}_\parallel}\zeta(\vec{r}_\parallel) \tag{12}$$

The local current density for the randomly rough electrode can be evaluated using Eq. (11) in Eq. (10), we obtain the current density expression upto second-order perturbation terms at a randomly rough surface is given by

$$\begin{aligned}j(p) = nF{\Lambda^0}_{a\Omega}[\hat{\mathcal{J}}_0(2\pi)^2\delta(K_\parallel) + \hat{\mathcal{J}}_1\,\hat{\zeta}(\vec{K}_\parallel) \\ + \hat{\mathcal{J}}_2\,\hat{\zeta}(\vec{K}'_\parallel)(\vec{K}_\parallel - \vec{K}'_\parallel);\ \vec{K}_\parallel \to \vec{r}_\parallel]\end{aligned} \tag{13}$$

where bracket notation for inverse Fourier transform is:

$$\{f(\vec{K}_\parallel); \vec{K}_\parallel \to \vec{r}_\parallel\} \equiv (1/(2\pi)^2)\int d^2K_\parallel \exp(\iota\vec{K}_\parallel.\vec{r}_\parallel) f(\vec{K}_\parallel).$$

The operators $\hat{\mathcal{J}}_0, \hat{\mathcal{J}}_1$ and $\hat{\mathcal{J}}_2$ are defined below

$$\hat{\mathcal{J}}_0 \equiv \left\{\frac{1}{\omega_0(\omega_0+\Lambda_{a\Omega})}\right\};$$

$$\hat{\mathcal{J}}_1 \equiv \left\{\frac{1}{\omega_0}\left(\frac{\omega_\parallel}{\omega_\parallel+\Lambda_{a\Omega}}-\frac{\omega_0}{\omega_0+\Lambda_{a\Omega}}\right)\right\}$$

$$\hat{\mathcal{J}}_2 \equiv \frac{1}{(2\pi)^2}\int d^2K_\parallel{}'\left\{\frac{1}{2}\left(\frac{\omega_0}{\omega_0+\Lambda_{a\Omega}}-\frac{\omega_\parallel}{\omega_\parallel+\Lambda_{a\Omega}}\right)+\frac{\omega_\parallel\omega_{\parallel,\parallel'}}{\omega_0(\omega_\parallel+\Lambda_{a\Omega})}-\frac{\omega_0}{\omega_{\parallel,\parallel'}+\Lambda_{a\Omega}}+\frac{\Lambda}{2\omega_0(\omega_0+\Lambda_{a\Omega})}\frac{K'_\parallel.(K_\parallel-K'_\parallel)}{\omega_\parallel+\Lambda_{a\Omega}}-\frac{\Lambda_{a\Omega}}{\omega_0(\omega_\parallel+\Lambda_{a\Omega})}\frac{K'_\parallel.(K_\parallel-K'_\parallel)}{\omega_{\parallel,\parallel'}+\Lambda_{a\Omega}}-\frac{|K_\parallel-K'_\parallel|^2}{\omega_0(\omega_{\parallel,\parallel'}+\Lambda_{a\Omega})}\right\}$$

The current density expression has three terms: the zeroth order term gives the response of a smooth electrode whereas the first- and second-order terms, i.e., second and third terms are responsible for the response arises due to random roughness of the electrode surface. The total current expression can be obtained by taking the surface integral of current density over the surface S_0 (i.e., z = 0). The Laplace transformed form of total current expression for a weakly and gently fluctuating surface is obtained as

$$I(p) = nF\Lambda^0{}_{a\Omega}\int_{S_o} d^2r_\parallel\left\{\hat{\mathcal{J}}_0(2\pi)^2\delta(K_\parallel)+\hat{\mathcal{J}}_1\hat{\zeta}(\vec{K}_\parallel)+\hat{\mathcal{J}}'_2\hat{\zeta}(\vec{K}'_\parallel)\hat{\zeta}(\vec{K}_\parallel-\vec{K}'_\parallel);\ \vec{K}_\parallel\to\vec{r}_\parallel\right\} \tag{14}$$

Here the operators $\hat{\mathcal{J}}_0$ and $\hat{\mathcal{J}}_1$ are same as in Eq. (13). The only difference is in the second order operator $\hat{\mathcal{J}}_2$ and $\hat{\mathcal{J}}'_2$ which is due to the area effect. The operator $\hat{\mathcal{J}}'_2$ is defined as

$$\hat{\mathcal{J}}'_2 \equiv \frac{1}{(2\pi)^2}\int d^2K_\parallel{}'\left\{\frac{1}{2}\left(\frac{\omega_0}{\omega_0+\Lambda_{a\Omega}}-\frac{\omega_\parallel}{\omega_\parallel+\Lambda_{a\Omega}}\right)+\frac{\omega_\parallel\omega_{\parallel,\parallel'}}{\omega_0(\omega_\parallel+\Lambda_{a\Omega})}-\frac{\omega_0}{\omega_{\parallel,\parallel'}+\Lambda_{a\Omega}}-\frac{\omega_\parallel}{2\omega_0(\omega_0+\Lambda_{a\Omega})}\frac{K'_\parallel.(K_\parallel-K'_\parallel)}{\omega_\parallel+\Lambda_{a\Omega}}-\frac{\Lambda_{a\Omega}}{\omega_0(\omega_\parallel+\Lambda_{a\Omega})}\frac{K'_\parallel.(K_\parallel-K'_\parallel)}{\omega_{\parallel,\parallel'}+\Lambda_{a\Omega}}-\frac{|K_\parallel-K'_\parallel|^2}{\omega_0(\omega_{\parallel,\parallel'}+\Lambda_{a\Omega})}\right\}$$

The inverse Laplace transform of Eq. (14) is an experimentally measurable quantity. It is important to realize that the second-order operators ($\hat{\mathcal{J}}_2$ and $\hat{\mathcal{J}}'_2$) in current density and total current expression, respectively are similar except one term. These operators provide details about the phenomenological characteristics of the diffusion-controlled adsorption problem, viz. diffusion characteristic by, ω_0, and adsorption characteristic by, $\Lambda_{a\Omega}$. Eqs. (13 and 14) emphasize the effect of roughness for an arbitrary surface profile.

2.1 *Admittance for arbitrary rough surface*

The admittance response at the interface of rough electrode needs to evaluate via the concentration field around the electrode profile. Kant et al. developed a series of models where the ab-initio methodology is used to solve the complex boundary conditions analytically.[38,46] The admittance expression for diffusion-limited adsorption process for randomly rough surface is expressed via Laplace transform of interfacial local current density ($j(t)$) as local admittance density ($y(\omega)$) and total current ($I(t)$) as total admittance ($Y(\omega)$), respectively under potentiostatic boundary constraints.[38,46] The expression relating local admittance density and current density is given by

$$y(\omega) = \frac{\iota\,\omega}{\eta_0}\,j(p=\iota\omega) = \frac{\iota\,\omega}{\eta_0}\int_0^\infty dt\; e^{-\iota\,\omega\,t}\,j(t) \tag{15}$$

The local admittance density expression for an arbitrary roughness surface profile, $\zeta(\vec{r}_\parallel)$, is obtained as the sum of various order terms in surface roughness, i.e., $\hat{\mathcal{Y}}_0$, $\hat{\mathcal{Y}}_1$ and $\hat{\mathcal{Y}}_2$[38,46] and is given by

$$y(\omega,\zeta(\vec{r}_\parallel)) = \frac{nFD\Lambda^0{}_{a\Omega}\,\omega_0^2}{\eta_0}\left\{\left[\hat{\mathcal{Y}}_0\,(2\pi)^2\,\delta(\vec{K}_\parallel)+\hat{\mathcal{Y}}_1\,\hat{\zeta}(\vec{K}_\parallel)+\hat{\mathcal{Y}}_2\,\hat{\zeta}(\vec{K}'_\parallel)\hat{\zeta}(\vec{K}_\parallel-\vec{K}'_\parallel)\right];\vec{K}_\parallel\to\vec{r}_\parallel\right\} \tag{16}$$

where the operators $\hat{\mathcal{Y}}_0$, $\hat{\mathcal{Y}}_1$ and $\hat{\mathcal{Y}}_2$ are given as

$$\hat{\mathcal{Y}}_0(\omega,\vec{K}_\parallel) \equiv \left\{\frac{1}{\omega_0(\omega_0+\Lambda_{a\Omega})}\right\};\ \hat{\mathcal{Y}}_1(\omega,\vec{K}_\parallel) \equiv \left\{\frac{1}{\omega_0}\left(\frac{\omega_\parallel}{\omega_\parallel+\Lambda_{a\Omega}}-\frac{\omega_0}{\omega_0+\Lambda_{a\Omega}}\right)\right\}$$

$$\hat{\mathcal{Y}}_2(\omega,\vec{K}_\parallel) \equiv \frac{1}{(2\pi)^2}\int d^2K'_\parallel\left\{\frac{1}{2}\left(\frac{\omega_0}{\omega_0+\Lambda_{a\Omega}}-\frac{\omega_\parallel}{\omega_\parallel+\Lambda_{a\Omega}}\right)+\frac{\omega_\parallel\omega_{\parallel,\parallel'}}{\omega_0(\omega_\parallel+\Lambda_{a\Omega})}-\frac{\omega_0}{(\omega_{\parallel,\parallel'}+\Lambda_{a\Omega})}+\frac{\Lambda_{a\Omega}}{2\omega_0(\omega_0+\Lambda_{a\Omega})}\frac{\vec{K}'_\parallel.(\vec{K}_\parallel-\vec{K}'_\parallel)}{(\omega_\parallel+\Lambda_{a\Omega})}-\frac{\Lambda_{a\Omega}}{\omega_0(\omega_\parallel+\Lambda_{a\Omega})}\frac{\vec{K}'_\parallel.(\vec{K}_\parallel-\vec{K}'_\parallel)}{(\omega_{\parallel,\parallel'}+\Lambda_{a\Omega})}-\frac{|\vec{K}_\parallel-\vec{K}'_\parallel|^2}{\omega_0(\omega_{\parallel,\parallel'}+\Lambda_{a\Omega})}\right\}$$

The local admittance density expression (Eq. 16)

extends the conventional representation of admittance density from smooth surface to arbitrary surface profile. The local admittance density expression provides a route for better understanding the processes such as aggregation, growth[22] and catalytic processes. The expression relating the total admittance with the total interfacial current via Laplace transformation is given by[43,46]:

$$Y(\omega) = \frac{\iota\,\omega}{\eta_0} I(p) = \frac{\iota\,\omega}{\eta_0} \int_0^\infty dt\; e^{-\iota\,\omega t}\, I(t) \tag{17}$$

The total admittance expression for an arbitrary roughness surface profile, $\zeta(\vec{r}_\parallel)$ in Laplace and Fourier transformed form is the sum of various-order terms. These terms are approximated upto second order in surface profile and is given by

$$\begin{aligned} Y(\omega, \zeta(\vec{r}_\parallel)) = \frac{nFD\Lambda^0{}_{a\Omega}\,\omega_0^2}{\eta_0} \int_{z=0} d^2 r_\parallel \Big\{ & \hat{\mathcal{Y}}_0\,(2\pi)^2\,\delta(\vec{K}_\parallel) \\ & + \hat{\mathcal{Y}}_1\,\hat{\zeta}(\vec{K}_\parallel) \\ & + \hat{\mathcal{Y}}_2'\,\hat{\zeta}(\vec{K}_\parallel')\hat{\zeta}(\vec{K}_\parallel - \vec{K}_\parallel'); \vec{K}_\parallel \to \vec{r}_\parallel \Big\} \end{aligned} \tag{18}$$

where the operator $\hat{\mathcal{Y}}_2'$ is defined as

$$\begin{aligned} \hat{\mathcal{Y}}_2'(\omega, \vec{K}_\parallel) \equiv & \frac{1}{(2\pi)^2} \int d^2 K_\parallel' \left[\frac{1}{2} \left(\frac{\omega_0}{\omega_0 + \Lambda_{a\Omega}} - \frac{\omega_\parallel}{\omega_\parallel + \Lambda_{a\Omega}} \right) \right. \\ & + \frac{\omega_\parallel \omega_{\parallel,\parallel'}}{\omega_0(\omega_\parallel + \Lambda_{a\Omega})} \\ & - \frac{\omega_0}{(\omega_{\parallel,\parallel'} + \Lambda_{a\Omega})} - \frac{\omega_\parallel}{2\omega_0(\omega_0 + \Lambda_{a\Omega})} \frac{\vec{K}_\parallel' . (\vec{K}_\parallel - \vec{K}_\parallel')}{(\omega_\parallel + \Lambda_{a\Omega})} \\ & \left. - \frac{\Lambda_{a\Omega}}{\omega_0(\omega_\parallel + \Lambda_{a\Omega})} \frac{\vec{K}_\parallel' . (\vec{K}_\parallel - \vec{K}_\parallel')}{(\omega_{\parallel,\parallel'} + \Lambda_{a\Omega})} - \frac{|\vec{K}_\parallel - \vec{K}_\parallel'|^2}{\omega_0(\omega_{\parallel,\parallel'} + \Lambda_{a\Omega})} \right] \end{aligned}$$

The operators $\hat{\mathcal{Y}}_2$ and $\hat{\mathcal{Y}}_2'$ has difference only in the numerical coefficient of the last term arises due to the projected area effect. Equation (18) generalizes the admittance expression for diffusion-controlled adsorption at random rough electrode in presence of uncompensated solution resistance. For some deterministic rough profile functions the generalized expression of admittance density and total admittance expression can be obtained using Eq. (16) and Eq. (18), respectively. With the help and understanding of the simple and extensively used technique of Fourier and Laplace transform, one can find out local admittance density and total admittance for arbitrary surfaces which play an important role in various aspects of diffusion-controlled adsorption processes in applied systems.

2.2 *Admittance for a random surface model*

In the random-surface model, characteristic features of surfaces are described by their statistical averages over various surface configurations. The ensemble-averaged admittance expression for diffusion-controlled adsorption can be obtained using the ab initio methodology.[38,46] The random surface profile of the interface can be assumed as a homogeneous stochastic function. For the centered Gaussian field, this surface structure factor is the Fourier transformed form of the two-point correlation function and is given by

$$\begin{aligned} \langle \hat{\zeta}(\vec{K}_\parallel) \rangle &= 0 \\ \langle \hat{\zeta}(\vec{K}_\parallel) \hat{\zeta}(\vec{K}_\parallel') \rangle &= (2\pi)^2 \delta(\vec{K}_\parallel + \vec{K}_\parallel') \langle |\hat{\zeta}(\vec{K}_\parallel)|^2 \rangle \end{aligned}$$

where $\langle |\hat{\zeta}(\vec{K}_\parallel)|^2 \rangle$ represents the power spectrum (PS) of roughness. Angular brackets demote the ensemble averaging over different possible surface configurations. The ensemble averaged admittance expression at the stationary, Gaussian random surface under diffusion-limited adsorption process in presence of uncompensated solution resistance is obtained as

$$\begin{aligned} < Y(\omega) > = Y_P(\omega) \Bigg[1 + \frac{\omega_0}{2\pi} \int_0^\infty dK_\parallel\, K_\parallel \Bigg[& \frac{\omega_\parallel - \omega_0}{(1 + \omega_\parallel L_{a\Omega})} \\ & + \frac{K_\parallel^2 L_{a\Omega}}{2(1 + \omega_0 L_{a\Omega})} \Bigg] \left\langle \left| \hat{\zeta}(\vec{K}_\parallel) \right|^2 \right\rangle \Bigg] \end{aligned} \tag{19}$$

where $L_{a\Omega} = \Gamma D(R_\Omega + 1/\iota\omega C_{ad})$, is the phenomenological adsorption-ohmic coupling length involving both adsorption and solution resistance parameters. Γ is the specific volume capacitance ($\Gamma = n^2F^2C_\alpha^0/RT$) and C_{ad} (=ΓK) is adsorption capacitance which is obtained due to the adsorption isotherm condition connected with linear diffusion. $Y_P(\omega)$ is the admittance expression at planar electrode for diffusion-limited adsorption process in presence of uncompensated solution resistance and is obtained as

$$Y_P(\omega) = \frac{A_0}{1/(\Gamma(\iota\omega D)^{1/2}) + R_\Omega + 1/(\iota\omega C_{ad})} \tag{20}$$

Here the Warburg admittance, $Y_W(\omega) = A_0\Gamma(\iota\omega D)^{1/2}$ and the adsorption admittance, $Y_{ad}(\omega) = \iota\omega C_{ad}$. The ensemble-averaged admittance expression for diffusion-limited adsorption process is proportional to the

projected area and a frequency-dependent complex dynamic roughness factor. All the morphological features of roughness are incorporated into the expression through the power spectrum. If the reaction does not involve adsorption process, under this limit it will approach the diffusion-limited process (Warburg admittance).[25] The physical problem of the effect of solution resistance, however, brings about a significant degree of deviation in the expected response.

2.3 *Admittance for realistic self-affine fractal surfaces*

Fractal model helps in understanding and explaining the complexity of natural and artificial surface topographies.[24,26,34,47–51] The surface model employed for rough electrodes and the interface is assumed to be a random surface. The roughness of these surfaces can be modeled approximately as self-affine fractals. The fractal nature of the electrode surface is limited by two cut-off lengths and shows the band-limited fractal behavior in this limited region. These self-affine band-limited fractals roughness is explained by the power-law PS.[24,26,34,47,49] SEM or AFM studies of the random surface help in obtaining the power spectrum of the rough electrode which widely represent the band-limited power law power spectrum and is given by

$$\left\langle \left| \hat{\zeta}(\vec{K}_{\parallel}) \right|^2 \right\rangle = \ell_{\tau}^{2D_H-3} |\vec{K}_{\parallel}|^{2D_H-7}, \quad 1/L \le |\vec{K}_{\parallel}| \le 1/\ell \tag{21}$$

The surface structure factor represents the statistically isotropic surfaces of a realistic fractal. The fractal morphological parameters of roughness are: fractal dimension (D_H), lower cutoff length (ℓ), upper cutoff length (L) and topothesy length (ℓ_τ). Fractal dimension is a global property which explains the scale invariance property of roughness. ℓ is the finest feature of electrode surface roughness. (L) and (ℓ) are the two limited length scales below and above which the surface shows fractal behavior, respectively. The ensemble-averaged admittance expression for an approximately self-affine isotropic fractal surface for diffusion-controlled adsorption in the presence of uncompensated solution resistance can be obtained by substituting Eq. (21) in Eq. (19) and solving resultant integral. The expression for a band-limited (isotropic) fractal PS is given by (for details see SI-B in supplementary information)

$$\langle Y(\omega) \rangle = Y_P(\omega)\,[1 + (\psi_1(\omega) + \psi_2(\omega))] \tag{22}$$

The first part of this expression shows the admittance contribution from a smooth surface and the second part reflects the roughness contribution to admittance for the band-limited isotropic fractal surface. The terms $\psi_1(\omega)$ and $\psi_2(\omega)$ can be expressed as

$$\begin{aligned}
\psi_1(\omega) &= [(A(\ell) - A(L)) - (H_1(\ell) - H_1(L))];\\
\psi_2(\omega) &= \frac{\mu\omega_0 L_{a\Omega}}{4\pi(\delta+1)(1+L_{a\Omega}\,\omega_0)}\\
&\quad \times \left\{ \frac{(\ell^{-2(\delta+1)} - L^{-2(\delta+1)})}{2} - \frac{H_2(\ell) - H_2(L)}{(1 - L_{a\Omega}\,\omega_0)} \right\}
\end{aligned} \tag{23}$$

where the integrals $A(u)$, $H_1(u)$ and $H_2(u)$ are obtained at ℓ and L and are given by

$$\begin{aligned}
A(u) &= \frac{\mu\omega_0^2}{4\pi\delta(1 - L_{a\Omega}\,\omega_0)} u^{-2\delta}\\
&\quad F_1\left[\delta; \frac{-1}{2}, 1; \delta+1; \frac{-D}{u^2\,\imath\omega}, \frac{DL_{a\Omega}^2}{u^2\,(D - L_{a\Omega}^2\,\imath\omega)}\right];\\
H_1(u) &= \frac{\mu\omega_0^2}{4\pi\delta(1 - L_{a\Omega}\,\omega_0)} u^{-2\delta}\\
&\quad {}_2F_1\left[1, \delta; \delta+1; \frac{DL_{a\Omega}^2}{u^2\,(D - L_{a\Omega}^2\,\imath\omega)}\right];\\
H_2(u) &= u^{-2(\delta+1)}\,{}_2F_1\left[1, \delta+1; \delta+2; \frac{DL_{a\Omega}^2}{u^2\,(D - L_{a\Omega}^2\,\imath\omega)}\right];
\end{aligned} \tag{24}$$

where $\delta = D_H - 5/2$, $F_1(\cdots)$ and ${}_2F_1(\cdots)$ represents the Appell[52] and hypergeometric,[53,54] functions, respectively which are numerically evaluated using Mathematica software. The variance in admittance expression (Eq. (22)) is the function of fractal morphological characteristics of roughness, i.e., $(D_H,\ \ell,\ L,\ \mu)$ and phenomenological complex diffusion layer (L_D) and adsorption-ohmic layer thickness $(L_{a\Omega})$. The extent of deviation in admittance response (from the smooth surface) is being influenced by the roughness of surface and adsorption kinetics.[55] As we approach the limit, $L_{a\Omega} \to 0$, i.e., complex adsorption-ohmic equilibration thickness vanishes, then $\psi_1(\omega)$ remains nonzero and gives Warburg admittance expression and $\psi_2(\omega)$ vanishes. One can analyze Warburg admittance[49] as a special case of diffusion-controlled adsorption admittance (Eq. (22)) under limit of, $L_{a\Omega} \to 0$. The various applications of diffusion-limited adsorption process with random roughness in applied systems make this theoretical model important and implementable one.

3. Results and Discussion

The theory developed here explicitly relates the impedance response of diffusion limited adsorption under influence of uncompensated solution resistance on rough finite fractal electrode. Theory is graphically analyzed with the adsorption isotherm parameter (K), uncompensated solution resistance (R_Ω) from medium and medium viscosity dependent diffusion coefficient (D). The influence of roughness at the electrode surface is characterized in terms of D_H, ℓ and ℓ_τ.

3.1 *Influence of solution resistance*

The influence of ohmic (potential) drop on the impedance spectra of diffusion-limited adsorption and electron transfer process at random finite fractal (rough) surface is calculated. Figure 2 shows the effect of solution resistance on the double logarithmic plot of the magnitude of impedance and phase response for rough surface. The impedance response is significantly influenced in the high frequency region with the variation in solution resistance, thus delaying the onset of the diffusion-controlled process. The enhancement in the magnitude of impedance is observed with rise in R_Ω. The impedance and phase plots show that as we increase the R_Ω, the intermediate anomalous regime with a hump diminishes. The morphological features of roughness are attributed to the hump in the magnitude and phase plots which is characteristic of roughness at the electrode surface.[11]

In the presence of uncompensated solution resistance, these features do not show up due to adsorption-ohmic equilibration thickness ($L_{a\Omega}$). From the phase plot, it is observed that the magnitude of phase angle decreases as the solution resistance increases. However, when solution resistance comes into play the phase angle shows a crossover to 0° towards higher frequency and 90° towards lower frequency. In the intermediate frequency regime, the phase angle plot shows the shift in the crossover frequency with rise in the value of uncompensated solution resistance. These graphs show a pseudo-kinetic control setting in the impedance response. This pseudo-kinetics is governed by the external parameters such as resistivity and the distance between working and reference electrodes. For low-frequency limit ($\omega \leq \omega_o$) and high frequency limit ($\omega \geq \omega_i$) the impedance response is adsorption controlled and ohmic controlled, respectively. In between these crossover frequencies, the anomalous regime exhibit approximately phase gain angle behavior. The inset shows in phase plot the

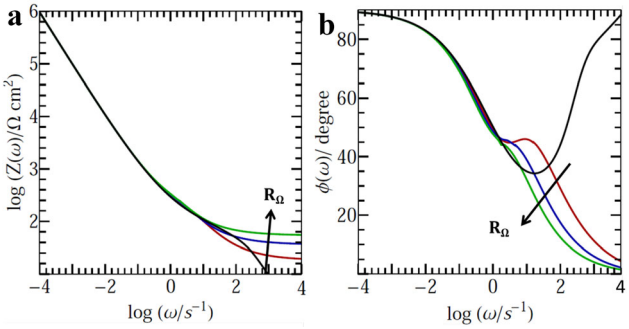

Figure 2. Effect of solution resistance on (a) double logarithmic plot of magnitude of impedance vs frequency and (b) phase plot. The value of R_Ω is varied as 10, 20, 30 Ω cm^2. Other fixed parameters used are: $D_H = 2.3$, $\ell = 30$ nm, $\ell_\tau = 600$ nm, $A_0 = 0.08\,\text{cm}^2$, $K = 20\,\mu$m, $D = 4 \times 10^{-6}$ cm^{2}s^{-1} and $C_O = C_R = 5$ mM. Black curve represents the response obtained at $R_\Omega = 0$.

characteristic hump for diffusion-limited adsorption without ohmic losses which are either delayed or completely curtailed in presence of increasing solution resistance. The essential feature is again the dynamic interplay of phenomenological lengths in question, i.e., adsorption ohmic length ($L_{a\Omega}$) and diffusion layer thickness (D/ω).

3.2 *Influence of diffusion coefficient*

The effect of variation of diffusion coefficient (with change in viscosity of medium) is observed on the double logarithmic plot of the magnitude of impedance vs frequency (Figure 3a) and phase plot (Figure 3b). It is observed that as the value of D increases the magnitude of impedance decreases. Adsorption phenomenon has been ascribed to the chemical changes on the bulk of the solution or the interface. But many observed frequency-variations cannot be explained in this way. Changing the diffusion coefficient alters the yardstick or diffusion length ($\sqrt{D/\omega}$) at the interface and hence the conception of various phenomena at the interface. These graphs show that as the diffusion becomes more sluggish, the uncompensated resistance becomes less influential in impedance response.

For a lower value of D, the diffusion sets up at a shorter frequency decoupling it from solution resistance effects at a longer frequency. Such values of diffusion coefficient are typical of the glycerol-based system, hexane based systems or concentrated glucose solutions. The roughness features in such situations can manifest themselves at intermediate frequency

giving anomalous response as observed in the transition graphs. The variation in the diffusion coefficient marks the transition from the non-viscous to the viscous system. One can see that as we increase the viscosity of the system, the roughness features at the interface are more perceptible. The phase angle in lower frequency regime enhances with increase in diffusion coefficient (or with decrease in viscosity of the medium). Decrease in the viscosity of the medium leads to suppression in the anomalous intermediate frequency valley and peak in impedance phase plot. This anomaly is due to emergence of pseudo-quasi-reversibility (e.g. $\phi \leq 45^0$) and anomalous Warburg response (e.g. $\phi \geq 45^0$). The phase peak shifts towards low frequency for less viscous medium, indicating suppression of diffusion control region.

3.3 *Influence of adsorption parameter*

The effect of linearized adsorption parameter (K) on diffusion-limited adsorption problem in presence of uncompensated solution resistance is observed on the log-log plot of the magnitude of impedance vs frequency (Figure 4a) and phase plot (Figure 4b). The influence of adsorption isotherm parameter is dominantly observed in the low-frequency region. The magnitude of impedance decreases with an increase in the value of K, in the low frequency-regime. It merges in the intermediate frequency regime and does not have any influence in the high-frequency region. From the phase plot, it is observed that the magnitude of the phase angle suppresses with the increase in adsorption isotherm parameter, K. It can be seen from this plot that the presence of adsorption with linear diffusion gives rise to capacitive behavior and can be seen towards lower frequency (in case of resistance controlled system phase angle approaches to 0° in the high-frequency regime).

It is concluded that the larger value of adsorption isotherm parameter, K, system will be more close to diffusion regime and a smaller value of adsorption isotherm parameter, K, system will be more close to adsorption. The low-frequency regime is controlled by adsorption kinetics and the high-frequency regime is limited by ohmic parameters. So it is clear that adsorption parameter, is a measure of diffusion-controlled adsorption process to diffusion-controlled process.

The three morphological features, i.e., fractal dimension, lower cut-off length and topothesy length dominantly control the electrochemical responses for a fractally rough surface. In the intermediate frequency regime, the plots show deviation in the impedance and phase response characteristic to the rough electrodes. Here we graphically represent the influence of various morphological features of roughness with solution resistance in the impedance and phase plots. The electrochemical response obtained by varying the morphological parameters and compared with the response of the planar electrode.

3.4 *Influence of fractal dimension*

The effect of varying fractal dimension (D_H) of roughness is observed on the log-log plot of magnitude of impedance vs frequency (Figure 5a) and phase plot (Figure 5b) in the presence solution resistance. It is seen that as the value of the D_H increases, the magnitude of impedance decreases. The low-frequency regime is the adsorption controlled regime. In the

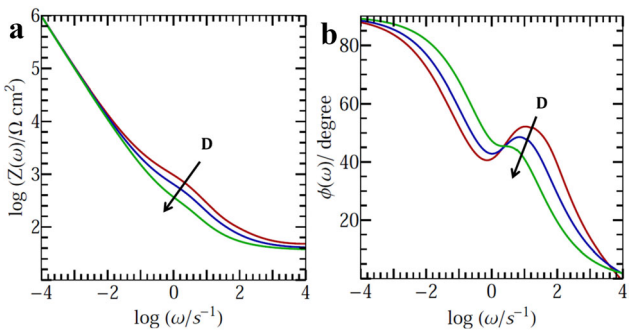

Figure 3. Effect of diffusion coefficient on (a) double logarithmic plot of magnitude of impedance vs frequency and (b) phase plot. The value of D is varied as (0.5, 1, 3)$\times 10^{-6}$cm$^2 s^{-1}$. Other fixed parameters used are: $D_H = 2.3$, $\ell = 30$ nm, $\ell_\tau = 600$ nm, $A_0 = 0.08\,\text{cm}^2$, $R_\Omega = 20\,\Omega\text{cm}^2$, $K = 20\ \mu$m and $C_O = C_R = 5$ mM.

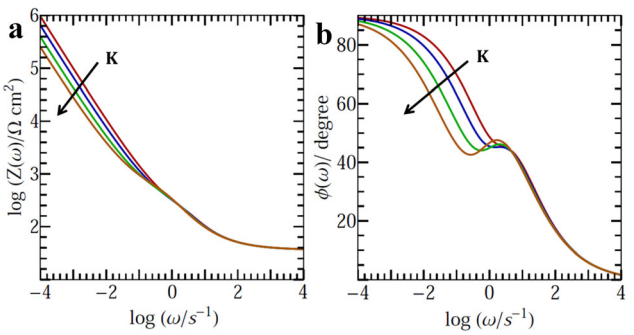

Figure 4. Effect of adsorption parameter on (a) double logarithmic plot of magnitude of impedance vs frequency and (b) phase plot. The value of K is varied as 20, 30, 50, 80 μm. Other fixed parameters used are: $D_H = 2.3$, $\ell = 30$ nm, $\ell_\tau = 600$ nm, $A_0 = 0.08\,\text{cm}^2$, $R_\Omega = 20\,\Omega\text{cm}^2$, $D = 4 \times 10^{-6}$ cm^{2}s^{-1} and $C_O = C_R = 5$ mM.

intermediate frequency region, the power-law impedance response is observed which is the characteristic of the dynamic response to surface roughness. This region is controlled by the mixing of diffusion and adsorption processes with the roughness of the surface. The slope of the power-law region varies with the variation in D_H, representing the strong dependence of anomalous response on the D_H. Here the outer and inner cut-off frequency are influenced by the solution resistance and fractal dimension, respectively. The sensitivity towards roughness is observed at higher frequencies in the presence of uncompensated resistance.

In the phase plot, it is observed that the phase value of minimum decreases with an increase in the value of D_H which enhances the pseudo-quasireversibility whereas the phase value of maximum enhances with rise in the value of D_H showing the anomalous Warburg behavior ($\phi \geq 45°$). The crossover in the intermediate frequency region is the point where $\phi = 45°$, showing Warburg behavior. There is no minimum and maximum is observed in the planar response depicting that these minimum and maximum results due to the roughness of the electrode. In the low-frequency region, phase angle tends towards 90° and in the high-frequency regime, it goes to 0° characteristic of the adsorption and solution resistance, respectively. There is a sharp fall in the value of phase angle in the high-frequency regime and ultimately reaches at 0°, this region is dominantly controlled by the solution resistance. This crossover from 0° to 90° is affected by the variation in the fractal dimension.

3.5 *Influence of lower cut-off length of fractal roughness*

The influence of varying lower cut off length (ℓ) of fractal nature is observed on the double logarithmic plot of the magnitude of impedance vs frequency (-Figure 6a) and phase plot (Figure 6b). The lower length scale represents the finest feature of surface fractal roughness. It is seen that as the value of ℓ increases there is an enhancement in the magnitude of impedance.

The effect of this morphological parameter is, however, propagated to a larger frequency window in the plots. It is evident that ℓ not just affects the higher frequencies but also influences the intermediate power-law response to a larger extent showing that the strongly dependent on the lower length scale cut off. The change in the slope of the curve is, however, enhanced in the presence of electrolytic resistance in the higher frequency ranges. The phase plot also shows a higher sensitivity towards the lower cut-off length. The deviation from the planar response is quite significant in the intermediate frequency regime. Decrease in the magnitude of finest length scale of roughness (ℓ) causes suppression in the magnitude of phase angle (in low frequency regime). This is followed by a rapid decrease in phase and trough formation in the intermediate frequency regime. Phase gain in the intermediate region becomes more prominent ℓ decreases. This crossover in the intermediate frequency region has unusual transition from pseudo-quasi-reversible to anomalous Warburg behavior. At very high frequency all the responses merge together with zero phase value.

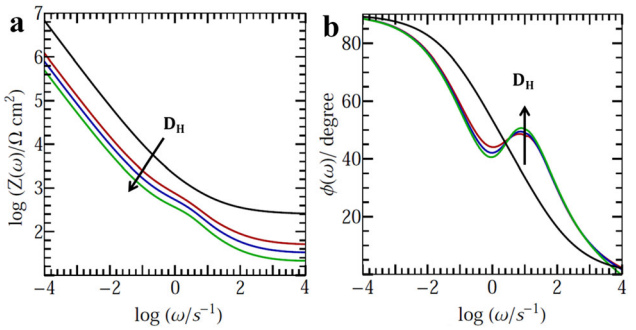

Figure 5. Effect of fractal dimension on (a) double logarithmic plot of magnitude of impedance vs frequency and (b) phase plot. The value of D_H is varied as 2.2, 2.3, 2.4. Other fixed parameters used are: $D = 3 \times 10^{-6}$ cm^2/s, $\ell =$ 30 nm, $\ell_\tau = 600$ nm, $A_0 = 0.08$ cm^2, $L = 10\,\mu$m, $K = 20\,\mu$m, $R_\Omega = 20\,\Omega$cm^2. Black curve shows the response of planar electrode.

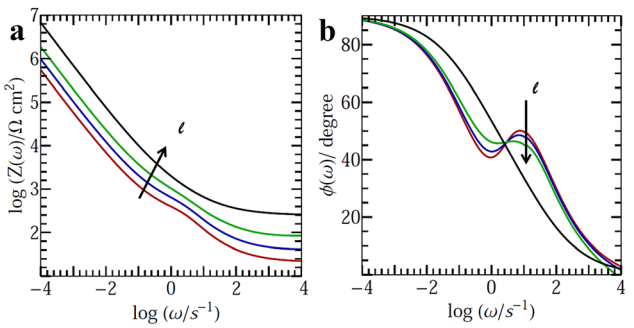

Figure 6. Effect of lower cut-off length on (a) double logarithmic plot of magnitude of impedance vs frequency and (b) phase plot. The value of ℓ is varied as 20, 30, 50 nm. Other fixed parameters used are: $D = 3 \times 10^{-6}$ cm^2/s, $D_H = 2.3$, $\ell_\tau = 600$ nm, $L = 10\,\mu$m, $K = 20\,\mu$m, $A_0 = 0.08$ cm^2, $R_\Omega = 20\,\Omega$cm^2. Black curve shows the response of planar electrode.

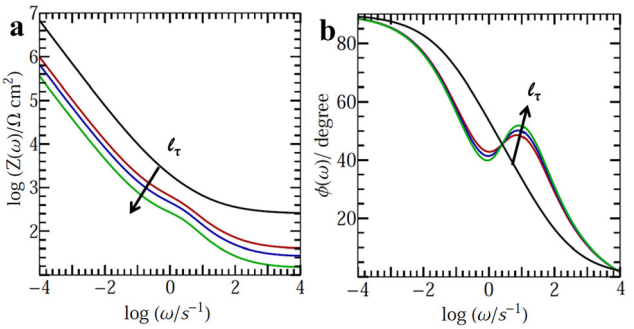

Figure 7. Effect of topothesy length on (a) double logarithmic plot of magnitude of impedance vs frequency and (b) phase plot. The value of ℓ_τ is varied as 0.2, 0.8, 1.2 μm. Other fixed parameters used are: $D = 3 \times 10^{-6}$ cm^2/s, $D_H = 2.3$, $\ell = 30$ nm, $L = 10\,\mu$m, $K = 20\,\mu$m, $A_0 = 0.08$ cm^2, $R_\Omega = 20\,\Omega$cm^2. Black curve shows the response of planar electrode.

3.6 *Influence of topothesy length*

Figure 7 represents the influence of varying width of surface roughness or topothesy length (ℓ_τ) on the log-log plot of the magnitude of impedance vs frequency and phase plot. It follows a similar behavior as that of the fractal dimension (D_H) and inverse behavior as given by lower cut-off length (ℓ). In the physical sense, ℓ_τ is the function of topothesy of a fractal which directly relates it to the width of interface. Greater the width of the interface, longer is the frequency span over which the roughness features are sensed.

4. Conclusions

The master equation derived for the admittance, i.e., Eq. (19), represents the dynamics of diffusion-limited adsorption process followed by charge transfer under influence of uncompensated solution resistance on a randomly rough electrode. The general power spectrum of the roughness is taken as homogeneous Gaussian random process. Equation (20) is for the admittance of diffusion-limited adsorption process in presence of uncompensated solution resistance but without electrode surface roughness. The fractal nature of roughness is expressed through Eq. (22) which describes the ensemble averaged admittance response for the finite (isotropic) fractal with a band-limited power spectrum. The first part of the equation represents the admittance contribution of smooth surface and the second part reflects the fractal dimension, topothesy length and finest scale of fractal roughness dependent response. This equation is used for generating the quantitative response curves. Our analysis shows that the impedance response at fractal electrode is influenced by the viscosity of medium through diffusion coefficient of electroactive species (D), solution resistance (R_Ω), adsorption isotherm (K) and finite fractal morphology parameters (e.g. D_H, ℓ_τ and ℓ). Following conclusions are obtained from the investigation:

1) The influence of solution resistance and adsorption process is governed through the phenomenological adsorption-ohmic-diffusion coupling length ($L_{a\Omega}$). This length operates at the terminal frequencies of the impedance spectra yielding the typical capacitive behavior ($\phi(\omega) \sim 90°$) at the lower frequencies identifiable with adsorption phenomenon and decays to resistance control ($\phi(\omega) \sim 0°$) at the higher frequencies.
2) The impedance response in high-frequency regime is governed by the uncompensated solution resistance along with the gross roughness factor. It is dominantly influenced by the diffusion coefficient or viscosity of medium and finite fractal features of roughness. So, the intermediate frequency regime largely influenced with the values of D_H, ℓ and ℓ_τ.
3) As the value of R_Ω increases, there is an enhancement in the value of L_Ω, which shifts the outer crossover (ω_o) frequency towards lower frequencies. Inner crossover frequency $\omega_i \approx D/(L_{a\Omega}^2 + \ell_\tau^2)$ is observed towards lower frequency and outer crossover frequency $\omega_o \approx D/L_{a\Omega}^2$ is observed towards high frequency.
4) In the presence of the adsorption phenomenon along with sizeable solution resistance, anomalous behavior is not observed even for a sufficiently rough surface.
5) Inner crossover frequency on the other extreme depends upon the value of adsorption isotherm parameter K. An increase in K denotes the weaker adsorption which causes a shift towards lower frequency. Inner crossover frequency $\omega_i \approx D/(L_{a\Omega}^2 + \ell_\tau^2)$ (for $L \geq h$) or $D/(L_{a\Omega}^2 + L^2)$ (for $L \leq \ell_\tau$) is observed towards lower frequency.
6) The solution resistance can limit the interpretation of adsorption dynamics on rough electrodes. The impedance phase response in intermediate region can show anomalous dilation, delay or completely curtail characteristic response.

Finally, the theory presented here successfully offers an understanding of impedance response for diffusion-limited adsorption processes under the influence of solution resistance at finite fractal electrodes. The electrochemical response obtained show sensitivity

towards electrode rough surface and also show anomalous response in the specific regime.

Supplementary Information (SI)

SIA-SI-B are available at www.ias.ac.in/chemsci.

Acknowledgements

Authors show their gratitude towards University of Delhi, India and DST-SERB, India (EMR/2016/007779) for financial support.

References

1. Dabrowski A 2001 Adsorption-from theory to practice *Adv. Colloid Interface Sci.* **93** 135
2. Feng J J, Xu J J and Chen H Y 2007 Direct electron transfer and electrocatalysis of hemoglobin adsorbed on mesoporous carbon through layer-by-layer assembly *Biosens. Bioelectron.* **22** 1618
3. Urbanova V, Karlicky F, Matěj A, Šembera F, Janoušek Z, Perman J A, Ranc V, Čepe K, Michl J, Otyepka M and Zbořil R 2016 Fluorinated graphenes as advanced biosensors effect of fluorine coverage on electron transfer properties and adsorption of biomolecules *Nanoscale* **8** 12134
4. Amemiya S 2020 Nanoelectrochemistry of adsorption-coupled electron transfer at carbon electrodes *Nanocarbon Electrochem.* 1
5. Wang C H, Yang C, Song Y Y, Gao W and Xia X H 2005 Adsorption and direct electron transfer from hemoglobin into a three-dimensionally ordered macroporous gold film *Adv. Funct. Mater.* **15** 1267
6. Qiu H, Xu C, Huang X, Ding Y, Qu Y and Gao P 2008 Adsorption of Laccase on the surface of nanoporous gold and the direct electron transfer between them *J. Phys. Chem. C* **112** 14781
7. Gmucova K 2012 A review of non-Cottrellian diffusion towards micro- and nano structured electrode, in: M Shao and Y Stegun (Eds.) *Electrochemical Cells New Advances in Fundamental Researches and Application* (Croatia: InTech) Ch. 1
8. Gauthier J A, Fields M, Bajdich M, Chen L D, Sandberg R B, Chan K and Norskov J K 2019 Facile electron transfer to CO_2 during adsorption at the metallsolution interface *J. Phys. Chem. C* **123** 29278
9. Giona M, Giustiniani M and Ludlow D K 1995 Influence of geometry and energetic heterogeneity of adsorption isotherms *Fractals* **3** 235
10. Ehrburger-Dolle F 1994 Some new correlations between Dubinin-Radushkevich and Freundlich equations and fractal dimension of microporous solids *Langmuir* **10** 2052
11. Kumar R and Kant R 2013 Admittance of diffusion limited adsorption coupled to reversible charge transfer on rough and finite fractal electrodes *Electrochim. Acta* **95** 275
12. Hanson E L, Schwartz J, Nickel B, Koch N and Danisman M F 2003 Bonding self-assembled, compact organophosphonate monolayers to the native oxide surface of silicon *J. Am. Chem. Soc.* **125** 16074
13. Thissen P, Vega A, Peixoto T, Chabal Y J, Chen X and Luais E 2012 Controlled, Low-coverage metal oxide activation of Silicon for organic functionalization: unraveling the Phosphonate bond *Langmuir* **28** 17494
14. Frumkin A N and Gaikazyan V I M 1951 Determination of the kinetics of adsorption of organic substances by a.c. measurements of the capacity and the conductivity at the boundary: Electrode-solution *Dokl. Akad. Nauk SSSR* **77** 855
15. Delahay P and Fike C T 1958 Adsorption kinetics with diffusion control-the plane and the expanding sphere *J. Am. Chem. Soc.* **80** 2628
16. Oliveira-Brett A M, da Silva L A and Brett C M A 2002 Adsorption of guanine, guanosine, and adenine at electrodes studied by differential pulse voltammetry and electrochemical impedance *Langmuir* **18** 2326
17. Martin M H and Lasia A 2011 Influence of experimental factors on the constant phase element behavior of Pt electrodes *Electrochim. Acta* **56** 8058
18. Giona M and Giustiniani M 1996 Thermodynamics and kinetics of adsorption in the presence of geometric roughness *Sep. Technol.* **6** 99
19. Sharma N, Goswami N and Kant R 2017 Experimental corroboration of the theory of Chronoamperometry at high roughness electrode for reversible charge transfer *J. Electroanal. Chem.* **788** 83
20. Chowdhury N R and Kant R 2018 Theory of generalized Gerischer impedance for quasi-reversible charge transfer at rough and finite fractal electrodes *Electrochim. Acta* **281** 445
21. Goswami N and Kant R 2019 Theory for impedance response of grain and grain boundary in solid state electrolyte *J. Electroanal. Chem.* **835** 227
22. Dhillon S, Goswami N and Kant R 2019 Theory for local EIS at rough electrode under diffusion controlled charge transfer: Onset of whiskers and dendrites *J. Electroanal. Chem.* **840** 193
23. Kant R and Singh M B 2017 Theory of the electrochemical impedance of mesostructured electrodes embedded with heterogeneous micropores *J. Phys. Chem. C* **121** 7164
24. Kumar R and Kant R 2009 Generalized Warburg impedance on realistic self-affine fractals: Comparative study of statistically corrugated and isotropic roughness *J. Chem. Sci.* **121** 579
25. Srivastav S and Kant R 2011 Anomalous Warburg impedance: Influence of uncompensated solution resistance *J. Phys. Chem. C* **115** 12232
26. Kant R and Kumar R 2009 Theory of generalized Gerischer admittance of realistic fractal electrode *J. Phys. Chem. C* **113** 19558
27. Kumar M, Srivastav S and Kant R 2020 Influence of electrode roughness on DC biased admittance of quasi-reversible charge transfer with uncompensated solution resistance *J. Electroanal. Chem.* **877** 114609
28. Islam Md M and Kant R 2011 Generalization of the Anson equation for fractal and non fractal rough electrodes *Electrochim. Acta* **56** 4467
29. Kant R and Islam Md M 2010 Theory of absorbance transients of an optically transparent rough electrode *J. Phys. Chem. C* **114** 19357

30. Chowdhury N R, Kumar R and Kant R 2017 Theory for the Chronopotentiometry on rough and finite fractal electrode: Generalized Sand equation *J. Electroanal. Chem.* **802** 64
31. Kumar M, Mishra G K and Kant R 2019 Theory for admittance voltammetry of reversible two step electron transfer process with DC bias at rough and fractal electrode *Electrochim. Acta* **327** 135024
32. Parveen and Kant R 2016 General theory for pulse voltammetric techniques at rough electrodes: Multistep reversible charge transfer mechanism *Electrochim. Acta,* **220** 475
33. Parveen and Kant R 2016 General theory for pulse voltammetric techniques on rough and finite fractal electrodes for reversible redox system with unequal diffusivities *Electrochim. Acta* **194** 283
34. Jha S K, Sangal A and Kant R 2008 Diffusion-controlled potentiostatic current transients on realistic fractal electrodes *J. Electroanl. Chem.* **615** 180
35. Kant R 1997 Diffusion-limited reaction rates on self-affine fractals *J. Phys. Chem. B* **101** 3781
36. Kant R 2010 General theory of arbitrary potential sweep methods on an arbitrary topography electrode and its application to random surface roughness *J. Phys. Chem. C* **114** 10894
37. Jha S K and Kant R 2010 Theory of potentiostatic current transients for coupled catalytic reaction at random corrugated fractal electrode *Electrochim. Acta* **56** 7266
38. Kant R and Rangarajan SK 1995 Diffusion to rough interfaces: finite charge transfer rates *J. Electroanal. Chem.* **396** 285
39. Srivastav S and Kant R 2010 Theory of generalized Cottrellian current at rough electrode with solution resistance effects *J. Phys. Chem. C* **114** 10066
40. Kant R 1993 Can current transients be affected by the morphology of the nonfractal electrode? *Phys. Rev. Lett.* **70** 4094
41. Garciá-Jareno J J, Sanmatiaś A, Navarro-Laboulais J and Vicente F 1999 Chronoamperometry of prussian blue films on ITO electrodes: Ohmic drop and film thickness effect *Electrochim. Acta* **44** 4753
42. Tacconi N R, Calandra A J and Arvia A J 1973 A contribution to the theory of the potential sweep method: charge transfer reactions with uncompensated cell resistance *Electrochim. Acta* **18** 571
43. Bard A J and Faulkner L R 1980 Electrochemical methods: Fundamentals and applications, Wiley, NY
44. Delahay P and Trachtenberg I 1957 Adsorption kinetics and electrode processes *J. Am. Chem. Soc.* **79** 2355
45. Lorenz W 1955 About the influence of surface roughness and potential determining ion adsorption on electrodes on the echo of diffusion polarization at constant current *Z. Elektrochem.* **59** 730
46. Kant R and Rangarajan S K 2003 Effect of surface roughness on interfacial reaction-diffusion admittance *J. Electroanal. Chem.* **552** 141
47. Jha S K and Kant R 2010 Theory of partial diffusion-limited interfacial transfer/reaction on realistic fractals *J. Electroanal. Chem.* **641** 78
48. Avnir D, Gutfraind R and Farin D 1994 *Fractals in Science* (Berlin, Germany: Springer-Verlag)
49. Kant R, Kumar R and Yadav V K 2008 Theory of anomalous diffusion impedance of realistic fractal electrode *J. Phys. Chem. C* **112** 4019
50. Pajkossy T 1991 Electrochemistry at fractal surfaces *J. Electroanal. Chem. Interfacial Electrochem.* **300** 1
51. Nyikos L, Pajkossy T, Borosy A P and Martemyanov S A 1990 Diffusion to fractal surfaces-IV. The case of the rotating disc electrode of fractal surface *Electrochim. Acta* **35** 1423
52. W N Bailey and A Stegan 1964 (Eds.) *Generalized hypergeometric Series* (New York and London: Stechert Hafner Service Agency)
53. M Abramowitz and I Stegan 1972 (Eds.) *Handbook of mathematical functions* (New York: Dover Publications Inc.)
54. Erdelyi A 1959 Hypergeometric functions of two variables *Acta Mathematica* **83** 131
55. Seri-Levy A and Avnir D 1993 Kinetics of diffusion-limited adsorption on fractal surfaces *J. Phys. Chem.* **97** 10380